

Biomechanical Comparison of Arthroscopic Repair Constructs for Meniscal Root Tears

Adam W. Anz,^{*†‡} MD, Eric A. Branch,[§] MS, and Justin D. Saliman,^{||} MD
*Investigation performed at the Andrews Research and Education Institute,
 Gulf Breeze, Florida, USA*

Background: Complete meniscal root tears render the meniscus nonfunctional. Repair constructs have been presented and tested; however, prior studies have evaluated suture patterns placed *ex vivo* without simulating an *in vivo* surgical setting. This study introduces a new double-locking loop suture pattern and compares its biomechanical properties and execution time with commonly used suture patterns. All constructs were performed using an all-inside arthroscopic technique.

Hypothesis: Complex suture repair constructs have higher failure loads, stiffness, and execution times compared with simple constructs.

Study Design: Controlled laboratory study.

Methods: Sutures were placed arthroscopically into the posterior horn root region of the medial and lateral menisci in 21 cadaveric knees. Four repair constructs were evaluated: 2 simple sutures (2SS), 1 inverted mattress suture (1MS), 1 double-locking loop suture (1DLS), and 2 double-locking loop sutures (2DLS). In total, 40 posterior meniscal roots were tested, with 10 trials for each construct. After arthroscopic placement of the root repair constructs, each meniscus was explanted and tested to failure on a uniaxial materials testing machine. The Kruskal-Wallis test was used to evaluate for the significance of maximum failure loads and stiffness between groups.

Results: The mean maximum failure loads were 137 ± 49 N (2SS), 126 ± 44 N (1MS), 186 ± 43 N (1DLS), and 368 ± 76 N (2DLS). Interconstruct comparison revealed a statistical difference between 2DLS and all 3 remaining constructs ($P < .01$) and 1DLS when compared with 2SS and 1MS ($P < .01$ for both). Statistical significance was not found between 2SS and 1MS ($P = .8$). The mean times for repair of the 4 fixation techniques were 1.8 ± 0.9 minutes (2SS), 2.4 ± 1.9 minutes (1MS), 4.7 ± 2.0 minutes (1DLS), and 5.4 ± 0.6 minutes (2DLS).

Conclusion: The double-locking loop suture repair technique had significantly higher failure loads compared with the 3 other methods tested. As the complexity of repair constructs increases, failure loads and surgical times increase.

Clinical Relevance: Complex suture patterns can be placed via an all-inside arthroscopic technique delivering higher failure loads for meniscal root repair with little increase in surgical time.

Keywords: meniscus; root tear; repair; failure load

*Address correspondence to Adam W. Anz, MD, Andrews Research and Education Institute, 1040 Gulf Breeze Parkway, Suite 203, Gulf Breeze, FL 32561, USA (adam.anz@andrewsortho.com).

†Andrews Orthopaedic and Sports Medicine Center, Gulf Breeze, Florida, USA.

‡Andrews Research and Education Institute, Gulf Breeze, Florida, USA.

§Florida State University College of Medicine, Tallahassee, Florida, USA.

||Cedars-Sinai Orthopaedic Center, Los Angeles, California, USA.

One or more of the authors has declared the following potential conflict of interest or source of funding: A.W.A. is a consultant for Ceterix Orthopaedics. J.D.S. is founder and chief medical officer for Ceterix Orthopaedics. He holds a patent related to the suture passing device. He is a consultant for Moximed. Funding for execution of this study was provided by Ceterix Orthopaedics.

The menisci play key roles in knee stability, proprioception, and load distribution.^{8,15,20,24} Central to these functions is the ability of the menisci to transfer compressive forces into hoop stresses. This ability to contain hoop stresses is substantially compromised in the event of a root tear, resulting in abnormal contact forces at the tibiofemoral articular surfaces.¹ A cadaveric load-distribution study illustrated contact pressures after medial root injuries that approximate those after total meniscectomy.¹² Left untreated, these injuries have been shown to result in progressive joint arthrosis.^{3,5} In addition, studies regarding the repair of root injuries have illustrated the ability of the repair to restore normal contact forces.^{1,6,12} The improved ability to recognize these injuries by magnetic resonance imaging and arthroscopic surgery, coupled with an ever-growing understanding of the deleterious consequences when left untreated, has resulted in the evolution of the technique for surgical repair.^{10,16}

Previous studies evaluating the failure properties of root repair techniques are limited.^{7,14,19} Native meniscal roots have high maximum failure loads, averaging 594 ± 241 N.¹⁴ Previous cadaveric studies have evaluated root repair constructs with maximum failure loads, defined as the maximum load achieved before displacement of the suture within meniscal testing tissue.^{14,19} Maximum failure loads have ranged from 58 to 191 N in such studies, dependent on the repair construct design. The more complex repair constructs are associated with higher maximum failure loads.^{14,19} While these previous studies have shed light on the failure properties of root repair constructs, these studies have limited clinical application because suture patterns were constructed *ex vivo* without simulating the surgical setting. These previously described complex suture patterns remain difficult to perform using open or arthroscopic techniques, as is routinely done clinically.^{9,21}

The goal of this study was to compare the failure properties of complex suture patterns via an all-inside arthroscopic technique with previously studied suture patterns.^{14,19} We hypothesized that the maximum failure load, stiffness, and repair execution time would vary among suture repair patterns, with higher values corresponding to increased complexity of the repair technique. We present and evaluate a new meniscal root repair construct placed with an all-inside arthroscopic technique. Evaluation of the failure properties and time for suture passage for different meniscal repair constructs may aid the clinician in decisions regarding optimal suture patterns for meniscal root repair.

MATERIALS AND METHODS

A total of 40 meniscal roots were utilized from 21 human cadaveric knee specimens. Five medial roots and 5 lateral roots were used for each suture repair group. We selected 10 specimens per group, as 8 specimens per group has proven sufficient and an accepted test size in previous biomechanical *in vitro* studies on meniscal suture techniques,^{7,14,17} and we confirmed this with a post hoc power analysis. The mean age of the specimens was 54 ± 5 years (range, 46-64 years); 17 menisci were from female donors, and 23 menisci were from male donors. Specimens were mounted to mimic a supine arthroscopic setup, with the knee free to move from 0° to 120° . Mounting the specimens involved exposing 3 inches of bone superior to the suprapatellar compartment and clamping in a 2-holed specimen clamp. Holes were drilled through the bone once provisionally placed in the clamp, and 2 metal rods were placed through the clamp and bone. In this simulated surgical position, varus and valgus stresses could be placed on the knee to open the medial and lateral compartments. Arthroscopic portals were created and diagnostic arthroscopic surgery performed. Evaluation of the knee to determine the competency of meniscal tissue was performed. Specimens exhibiting macroscopic articular cartilage defects equal or greater than Outerbridge III and/or meniscal degeneration or meniscal tears involving Cooper zones 0, 1, and/or 2 were excluded from the study.⁴ Two menisci

were excluded because of macroscopic degeneration on initial arthroscopic evaluation.

Sutures were passed arthroscopically into the posterior horn of the medial and lateral menisci adjacent to their root insertions with a technique identical to that used during *in vivo* clinical meniscal root tear repair. All sutures were passed with a newly available arthroscopic suture passing device (NovoStitch, Ceterix Orthopaedics Inc). The operation of the device, as well as potential repair constructs, has previously been reported.²³ The device has an upper articulating jaw that approximates the curvature of the femoral condyles and a lower retractable jaw that houses a passing needle. The procedure involved loading the passing needle with a suture and retracting the lower jaw. The device was inserted into the knee and the upper jaw positioned above the meniscus. The lower jaw was advanced and positioned under the meniscus. A lever advanced the needle, passing the suture through the meniscus and capturing the suture in the upper jaw. The lower jaw was retracted and the instrument removed from the knee (see Video Supplement). The shaft of the device was 2.8 mm in height. The upper jaw was 1.5 mm in height and 5 mm in width, the lower jaw was 1.7 mm in height and 3 mm in width, and the passing needle was flat, 0.3 mm in height, and 1.5 mm in width. Repair constructs included 2 simple sutures (2SS), 1 inverted mattress suture (1MS), 1 double-locking loop suture (1DLS), and 2 double-locking loop sutures (2DLS) (Figure 1). All repair constructs utilized No. 2 braided polyester and ultrahigh molecular weight polyethylene sutures (FiberWire, Arthrex Inc).

Simple suture passage involved passing a suture end directly from the tibial side of the meniscus to the femoral side. For the 2SS construct, this was performed twice: once within the peripheral meniscal root 8 mm from the root attachment and once approximately 5 mm central to the initial suture (Figure 1, A and B). Creation of the inverted mattress suture pattern involved 2 steps: passage of one free end of the suture 8 mm from the root attachment, followed by passage of the opposite end of the same suture 5 mm central to the initially passed limb (Figure 1, C and D). Creation of the double-locking loop suture construct involved 4 steps: (1) a free end of the suture was passed through the periphery of the meniscus (Figure 2A); (2) the opposite end of the same suture was then passed more centrally within the same anteroposterior vector as the previous end (Figure 2B); (3) the final pass involved passing the middle of the same suture through the apex of the meniscal root so that a loop was formed (Figure 2C); and (4) to complete the construct, the 2 suture ends from steps 1 and 2 were passed through the loop created in step 3 and pulled until the construct was reduced down to the meniscus (Figure 2D) (see Video Supplement). In the 1DLS group, the apex of the first suture construct was placed 5 mm from the root attachment point and the remaining limbs placed 10 mm from the root attachment point (Figure 1, E and F). In the 2DLS group, the first suture was placed as above, and the second suture was placed with the apex 5 to 10 mm from the first construct and the remaining limbs 10 to 15 mm from the first construct (Figure 1, G and H). Pie crusting of the

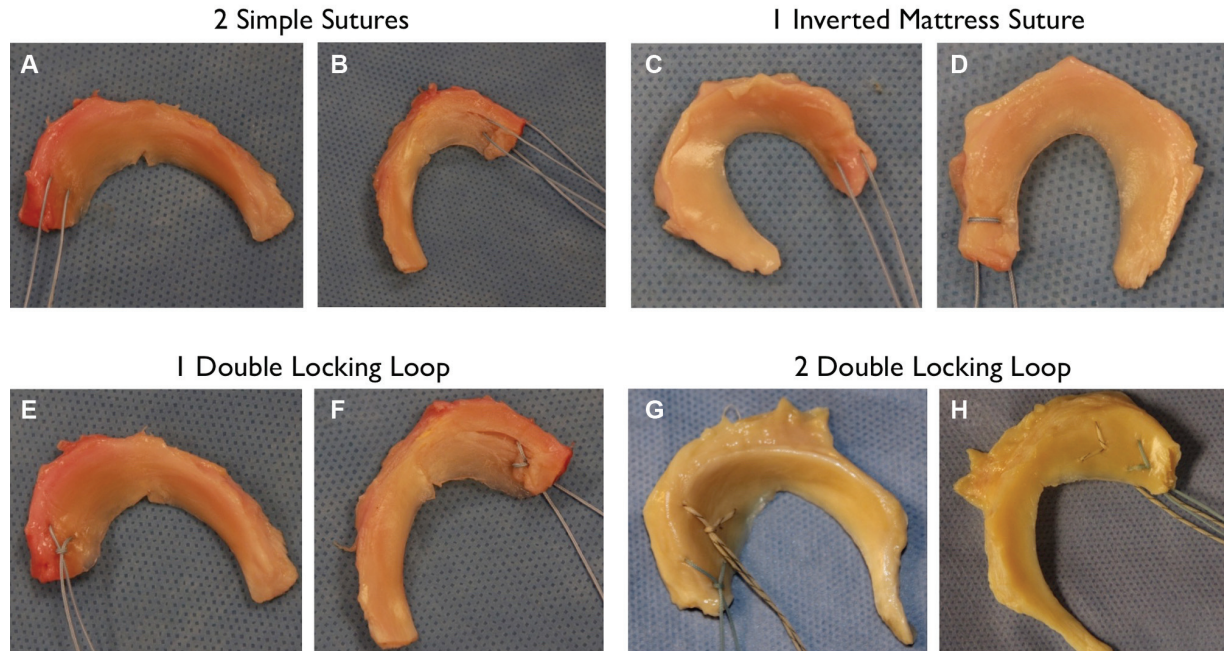


Figure 1. Meniscal repair constructs: (A, C, E, G) femoral views and (B, D, F, H) tibial views. (A, B) 2 simple sutures, (C, D) 1 inverted mattress suture, (E, F) 1 double-locking loop suture, and (G, H) 2 double-locking loop sutures.

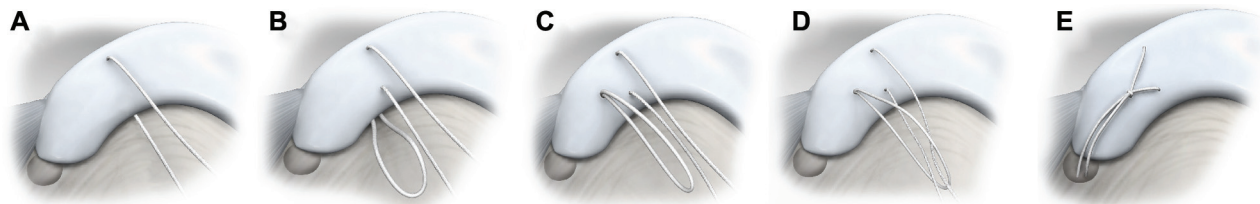


Figure 2. Double-locking loop suture construct. (A, B) Passage of the free ends of the suture. (C) The construct after passage of the loop created in A and B. (D) Passage of the free ends through the loop created. (E) The final construct with passage through the transosseous construct.

meniscotibial aspect of the deep medial collateral ligament was performed when necessary for access to the medial posterior root as previously described.¹¹ We found pie crusting necessary in most specimens for access to the medial root, although exact numbers were not recorded. This is similar to our clinical experience with the initial version of the suture repair device. The time to completion of each suture construct was recorded and defined as the time from instrument insertion to stitch completion. All other times for preparation, clearing the field, and root exposure were excluded.

After arthroscopic placement of the repair constructs, the knees were disarticulated, and the menisci were explanted using sharp dissection of the roots from their tibial attachments. Individual meniscus specimens were then tested to failure on a uniaxial materials testing machine (model 5565, Instron Corp) with a screw side action–grip specimen clamp (model 2710-102, Instron Corp) rated to 500 N. Specimens were kept moist using saline solution

and were tested within an hour of placement of the suture construct. A custom acrylic base plate with a meniscal trough and suture tunnel was used to replicate the trough and transosseous tibial tunnel utilized during meniscal root repair. Each specimen was initially mounted in the superior specimen mount in line with the circumferential fibers and lowered into the prefashioned trough of the acrylic base. Sutures were passed through the acrylic tunnel and tied over a 12-mm metal suture button (Arthrex Inc). Knot tying over the button involved 4 half-hitches thrown in an alternating fashion (Figure 3).

The tensile testing protocol included a preload period for 10 seconds, a preconditioning period with cyclic loading, and a period of load to failure. Throughout testing, the tensile load and displacement were recorded at 10 Hz. The preconditioning period involved 20 cycles from 50 to 100 N at 0.5 mm/s, and the period of load to failure involved an increase in force at a rate of 0.5 mm/s until failure. Through the entire testing process, the actuator's load

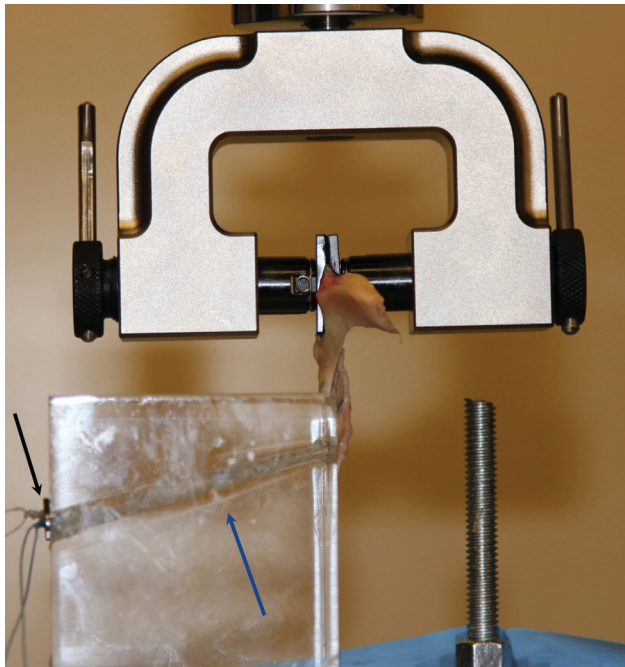


Figure 3. Uniaxial testing construct. The left arrow points to the suture button, and the right arrow points to the tunnel through an acrylic jig.

and displacement were captured and a displacement curve generated using mechanical testing software (Bluehill 2, Instron Corp). Maximum failure load was defined as the first loss of structural integrity illustrated by the initial peak on the load-displacement curve (Figure 4). Instances where suture slipping initiated and then halted were visible by multiple peaks in the load-displacement curve (Figure 4B). This occurred in 8 specimens. In these scenarios, the initial peak clearly demarcated the first loss of construct integrity, and the corresponding load was selected as the maximum failure load. Six specimens failed during the preconditioning cycle, including four 1MS constructs and two 2SS constructs. The failure loads of these specimens were included in the data calculations.

Specimens were monitored for slipping within the clamp visually during testing as well as on posttest analysis of the load-displacement curve to ensure that slipping of meniscal tissue within the clamp did not occur. Stiffness values were calculated for each construct before and after cyclic loading. Stiffness values were determined by calculating the slope of the load-displacement curve during initial loading of the construct from 50 to 100 N before cyclic loading and also after cyclic loading during load to failure from 50 N to 80% of the maximum failure load. Meniscus specimens were kept moist before and during testing.

All data were checked for normality of distribution, and a Kruskal-Wallis 1-way analysis of variance by ranks was chosen to evaluate for statistical significance of the maximum failure load and stiffness between groups, as the data were not distributed normally. In post hoc power analysis, the minimal detectable difference was determined using the observed sample effect size, assuming

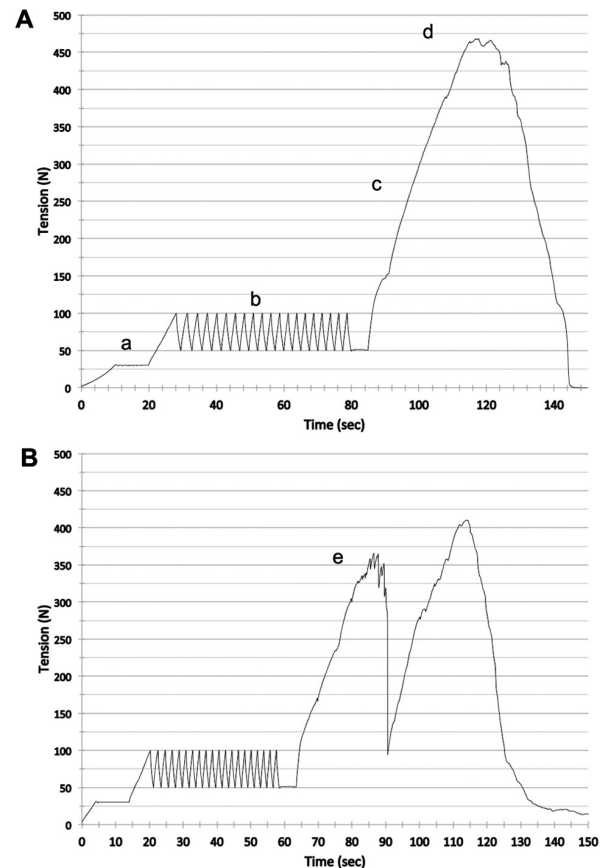


Figure 4. Load-displacement curves for uniaxial tension testing. (A) The load-displacement curve illustrates the period of preloading (a), period of cyclic loading (b), period of failure (c), and the maximum failure load (d). (B) Instances where suture slipping initiated and then halted were visible by multiple peaks in the curve. In these scenarios, the initial peak clearly demarcated the first loss of construct integrity, and the corresponding load was selected as the maximum failure load (e).

nonnormal distribution of data and keeping the type II error (β) at 20% and the type I error (α) $< .05$. Power calculations were performed using simulations in SAS version 9.2 (SAS Institute Inc).

RESULTS

The 2DLS repair construct exhibited the highest maximum failure load (Table 1). The 1DLS construct exhibited the second highest failure load, followed by 2SS and 1MS. Interconstruct comparison using the Kruskal-Wallis test revealed a statistical difference between 2DLS and all 3 remaining constructs ($P < .01$ for all 3) and 1DLS when compared with 2SS and 1MS ($P < .01$ for both). Statistical significance was not found between 2SS and 1MS ($P = .8$) (Figure 5). The failure mechanism for all specimens tested was suture pull-through of meniscal tissue, with the exception of 1 specimen in the 2DLS group in which the body of

TABLE 1
Results of Uniaxial Tension Testing^a

Construct	Failure Load, N	Preconditioning Stiffness, N/mm	Postconditioning Stiffness, N/mm	Repair Time, min
2 double-locking loop sutures	368 ± 76 (468-204)	20.8 ± 3.1 (28.1-16.9)	31.1 ± 5.0 (39.8-22.9)	5.4 ± 0.6 (6.5-4.8)
1 double-locking loop suture	186 ± 43 (251-132)	9.7 ± 2.1 (14.2-7.7)	21.9 ± 6.1 (30.6-13.6)	4.7 ± 2.0 (2.3-8.3)
2 simple sutures	137 ± 49 (258-68)	20.6 ± 4.1 (28.5-13.8)	31.5 ± 7.2 (44.4-21.8)	1.8 ± 0.9 (3.3-1.0)
1 inverted mattress suture	126 ± 44 (192-69)	11.7 ± 4.5 (18.8-4.0)	26.8 ± 5.8 (34.9-19.2)	2.4 ± 1.9 (3.2-0.8)

^aValues are presented as mean ± SD (range).

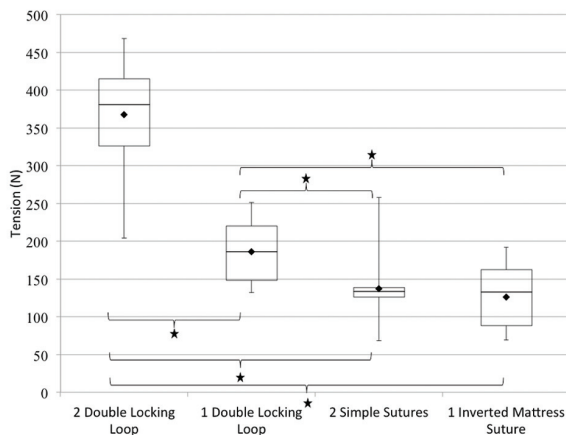


Figure 5. Box plot of the maximum failure load of 4 meniscal repair constructs. Brackets with stars represent statistically significant interconstruct comparison. The y-axis represents tension (in newtons).

the meniscus elongated and failed just distal to the specimen clamp. Power calculations determined that the minimal detectable between-group difference for the maximum failure load is equal to 67 N.

Precycling stiffness gave the following results. The 2DLS repair construct exhibited the highest preconditioning stiffness (Table 1). The 2SS construct exhibited the second highest preconditioning stiffness, followed by 1MS and 1DLS. The 2SS repair construct exhibited the highest postconditioning stiffness. The 2DLS repair construct exhibited the second highest, followed by 1MS and 1DLS. With precyclic stiffness, interconstruct comparison revealed a statistical difference between 2-suture and 1-suture constructs ($P < .05$), with the 2-suture constructs exhibiting increased mean values for stiffness. Statistical significance was not found in comparison among the 2-suture constructs or in comparison among the 1-suture constructs. With postcyclic stiffness, interconstruct comparison revealed a statistical difference between 2DLS and 1DLS as well as 1DLS and 2SS ($P < .05$) (Figure 6). All constructs revealed a statistical difference between precyclic and postcyclic stiffness ($P < .01$), with postcyclic stiffness exhibiting increased mean values for stiffness.

The mean times for repair of the 4 fixation techniques were 1.8 minutes (2SS), 2.4 minutes (1MS), 4.7 minutes

(1DLS), and 5.4 minutes (2DLS) (Table 1). Interconstruct comparison using the Kruskal-Wallis test revealed a statistical difference between 2DLS and all 3 remaining constructs ($P = .028$ [1DLS], $P < .01$ [2SS], and $P < .01$ [1MS]) and 1DLS when compared with 2SS and 1MS ($P < .01$ for both). Statistical significance was not found between 2SS and 1MS ($P = .60$).

DISCUSSION

This study evaluated the failure properties of suture constructs placed arthroscopically, mimicking repair of a meniscal root tear, to aid the clinician regarding suture placement. It also introduced a complex suture pattern of meniscal root repair, examining 2 unique applications of this pattern; each application demonstrated a greater maximum failure load than that of previously described constructs. The strongest construct had a mean pull-out strength of 368 N, and constructs composed of 2 sutures were stiffer than constructs composed of 1 suture. The study demonstrated approximately twice the time to construct complex suture repair patterns compared with simple patterns in a simulated arthroscopic environment.

The improved strength of the double-locking loop stitch is likely attributable to its ability to obtain cross-fiber tissue purchase within the posterior horn of the meniscus. It is also likely that use of a greater surface region of the posterior horn of the meniscus than may be possible with other techniques contributed to these results. Additional benefits of this construct might be present from the resultant downward vector of pull on the meniscal root into the prepared trough. This vector may improve the meniscal footprint's contact area and contact pressure, but additional study will be needed to evaluate this phenomenon and its importance.

The current study did not evaluate the native meniscal root strength, as 2 previous studies have evaluated the failure properties of the native meniscal root. Kopf et al¹⁴ examined all 4 meniscal root failure loads in 43 specimens with a mean age of 29.3 ± 12.2 years and reported a mean failure load of 678 ± 200 N for the posteromedial root and 648 ± 140 N for the posterolateral root. A recent similar study evaluated posteromedial root failure loads in 12 specimens with a mean age of 74 years, finding a mean of 359.5 ± 168.0 N.¹⁹ The strongest repair construct in this current study illustrated a mean failure load of 368 ± 76 N. The current study utilized a preconditioning cycle from 50 to 100 N, which is similar to the

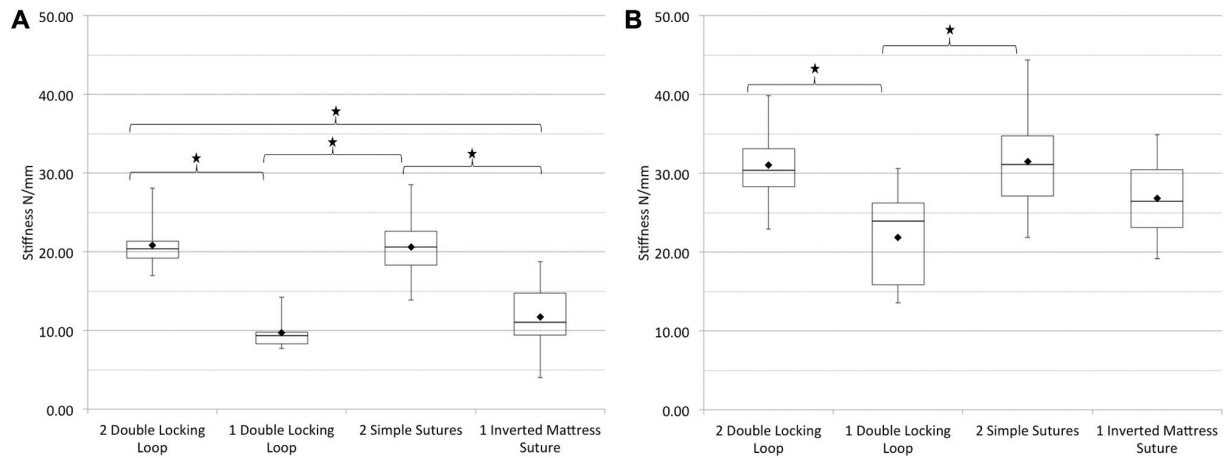


Figure 6. Box plot of the stiffness of 4 meniscal repair constructs. Brackets with stars represent statistically significant interconstruct comparison. (A) Preconditioning stiffness calculated by the slope of the displacement curve during initial loading of the construct from 50 to 100 N before cyclic loading. (B) Postconditioning stiffness calculated by the slope of the displacement curve during load to failure from 50 N to 80% of the maximum failure load. The y-axis represents tension (in newtons).

tensile testing regimen used by Kopf et al¹⁴ to assess the native root failure load. When evaluating suture repair, previous studies have used preconditioning cycles from 5 to 10 N or 5 to 20 N.^{7,14}

This study illustrated a higher failure load of 2SS (137 N) compared with the findings of Kopf et al¹⁴ and Mitchell et al¹⁹ (64 N and 96 N, respectively). Previous meniscal and rotator cuff repair studies have suggested that the characteristics of the puncturing device may likely have the greatest effect on tissue integrity during repair, with larger punctures likely having a negative effect on tissue integrity.^{14,22} However, the suture passer used in this study creates smaller punctures than that of a suture shuttling device, which may explain the difference in values of our simple suture constructs compared with previous studies.^{7,14} This difference might be also attributable to the freedom of suture placement, as the location of the stitches was not dependent on the location of a transtibial tunnel. This allowed the sutures to be effectively placed farther from the apex of the meniscal root than that possible in previous studies. The direct bottom-to-top passing vector may also have contributed to this effect. While it has been theorized that more complex patterns, which require multiple meniscal punctures, may promote suture cutouts, we did not observe this phenomenon, as more complex patterns proved stronger.

This study utilized No. 2 braided polyester and ultrahigh molecular weight polyethylene sutures, while Kopf et al¹⁴ utilized No. 2 high-strength polyethylene sutures (Ultrabraid, Smith & Nephew), and Mitchell et al¹⁹ utilized No. 0 braided polyester and ultrahigh molecular weight polyethylene sutures. Such a variance in suture composition and size likely affects pull-out strength and stiffness. In a biomechanical study, 6 braided polyester and ultrahigh molecular weight polyethylene sutures (FiberWire) have been shown to have a high maximum failure load and stiffness with low displacement when

compared with other suture materials in meniscal root repair. Additional comparative studies on suture placement within the posterior horn, needle size, needle shape, and suture material and size are warranted.

Although interstudy comparison is not exact, it is of interest. The inverted mattress suture passed in this study is similar to the loop stitch produced in the 2 previous *ex vivo* studies and approximated the other studies regarding failure loads (Table 2). The modified Kessler, in comparison, appears to have strength higher than those of loop and mattress patterns but not as high as locking loop constructs.¹⁴ The double-locking loop suture construct in this study illustrated a similar maximum failure load compared with the locking loop stitch studied by Mitchell et al.¹⁹ Placement of the 2DLS construct appears to have higher failure properties than those of all previously studied constructs, and most approach the strength of the native meniscal root (Table 2). It is also more relevant than previously studied locking loop constructs because it can be passed *in vivo*. A recent study has evaluated the tensile forces placed on root repair in a cadaveric model. A 500-N load placed at 90° of knee flexion creates approximately 60 N of tensile force on a root repair construct.²⁵ This magnitude of tension suggests that unrestricted motion or weightbearing could be sufficient to displace repair constructs created with simple suture patterns.

Stiffness is a measure of the ability of a construct to resist deformation when a force is applied. Previous studies^{2,13} have found no difference in stiffness of all-inside repair constructs among all-inside repair devices and *ex vivo* simple sutures. A recent meniscal root repair study⁷ using porcine menisci illustrated higher stiffness with a suture anchor construct when compared with a transtibial construct. Our study evaluated transtibial constructs alone. We found higher stiffness in 2-suture constructs compared with 1-suture constructs and in all suture constructs after cyclic conditioning. This study measured

TABLE 2
Comparison of Maximum Failure Loads (in Newtons) in This Study
With Failure Loads and Native Strength Reported in Previous Studies^a

Construct	Kopf et al ¹⁴	Mitchell et al ¹⁹	Present Study
Posteromedial root	678 ± 200	359.5 ± 168.0	
Posterolateral root	648 ± 140		
1 simple suture		58 ± 30	
2 simple sutures	64.1 ± 22.5	96 ± 51	137 ± 49
Loop suture	101 ± 42	120 ± 55	
Horizontal suture			126 ± 44
Modified Kessler	143 ± 33		
Locking loop stitch		191 ± 45	
1 double-locking loop suture			186 ± 43
2 double-locking loop sutures			368 ± 76

^aValues are presented as mean ± SD.

displacement and calculated stiffness based on actuator data from the mechanical testing machine. Although a previous study⁷ has utilized this method to determine displacement and stiffness, this method may lack exact displacement data. With the exception of 1 specimen in the 2DLS group, specimen slipping within the clamp was not observed. If not detected visually during testing, displacement through specimen slipping would have been evident on the load-displacement curve. Measuring displacement with markers and high-speed cameras after uniform pretension of button suture fixation could theoretically improve the testing model. Further study regarding complex suture patterns and suture anchor fixation would better refine the ideal repair technique.

This study did not completely reproduce the natural loads and stresses of the meniscus after root repair. Forces applied were uniaxial, while natural knee motion and loading produce vertical shear, radial extrusion, and axial compression. While the presented ex vivo comparison gives comparative insight between meniscal root repair constructs, it does not effectively determine the ability of these constructs to restore normal root failure properties or the effects of a complex suture pattern on meniscal kinematics and physiology. In the setting of 2DLS, we theorize that the effects on meniscal function would be minimal as the traction force of the suture on the posterior horn is spread while the vector of pull is focused on the apex of the meniscal root at the transosseous tunnel aperture. Further in vivo study would aid in analysis of in vivo stresses as well as contact areas and pressures. While an in vivo study would better capture the restoration of contact pressures and areas, the aim of this study was to compare the strength of different meniscal repair constructs in a simple and reproducible fashion.

A weakness of this study is the use of elderly cadaveric specimens, with a mean age of 54 years, in which meniscal repair is seldom indicated. Additionally, no data were available regarding the mechanical axis of these specimens. The mean age of the specimens was higher than those undergoing this procedure, as specimens younger than 40 years are rarely available. The use of porcine menisci may have provided more consistent samples; however, prior authors have noted difficulty with the use of

porcine meniscus specimens because of size.¹⁸ Our objective was to provide more data on human meniscal tissue as well as data on repair constructs placed arthroscopically instead of ex vivo. An additional weakness is the use of both medial and lateral meniscal tissue in each group, as this may be a confounding variable. However, a previous study has illustrated no difference between the native strength of posterior medial and posterior lateral roots.¹⁴ For this reason, it was determined that 5 medial menisci and 5 lateral menisci per sample group was acceptable. We did not test normal control specimens for 3 reasons. First, the uniaxial testing clamps were rated to 500 N, which is likely not sufficient.¹⁴ Second, values for normal controls have been previously published.^{14,19} Third, our primary goal was to determine which suture pattern was the strongest in an interconstruct comparison.

With a minimal detectable difference of 67 N, post hoc power analysis suggested that the study was adequately powered to determine the difference in maximum failure loads between 2DLS and the remaining groups. The type II error (β) for comparison of the 1DLS to the 2SS and 1MS groups was found to be >20%, suggesting that the study was slightly underpowered for this comparison.

CONCLUSION

Complex suture patterns including the double-locking loop stitch illustrate higher maximum failure loads and are clinically feasible. Additional study and evolving technology may advance our ability to successfully repair the torn meniscal root, enabling optimal preservation of the knee joint.

A Video Supplement for this article is available in the online version or at <http://ajsm.sagepub.com/supplemental>.

REFERENCES

- Allaire R, Muriuki M, Gilbertson L, Harner CD. Biomechanical consequences of a tear of the posterior root of the medial meniscus: similar to total meniscectomy. *J Bone Joint Surg Am*. 2008;90:1922-1931.

2. Barber FA, Herbert MA, Bava ED, Drew OR. Biomechanical testing of suture-based meniscal repair devices containing ultrahigh-molecular-weight polyethylene suture: update 2011. *Arthroscopy*. 2012;28:827-834.
3. Berthiaume MJ, Raynauld JP, Martel-Pelletier J, et al. Meniscal tear and extrusion are strongly associated with progression of symptomatic knee arthritis as assessed by quantitative magnetic resonance imaging. *Ann Rheum Dis*. 2005;64:556-563.
4. Cooper DE, Arnoczky SP, Warren RF. Meniscal repair. *Clin Sports Med*. 1991;10:529-548.
5. Fairbank TJ. Knee joint changes after meniscectomy. *J Bone Joint Surg Br*. 1948;30:664-670.
6. Feucht MJ, Grande E, Brunhuber J, et al. Biomechanical evaluation of different suture materials for arthroscopic transtibial pull-out repair of posterior meniscus root tears [published online September 3, 2013]. *Knee Surg Sports Traumatol Arthrosc*. doi:10.1007/s00167-013-2656-z.
7. Feucht MJ, Grande E, Brunhuber J, Rosenstiel N, Burgkart R, Imhoff AB. Biomechanical comparison between suture anchor and transtibial pull-out repair for posterior medial meniscus root tears. *Am J Sports Med*. 2014;42:187-193.
8. Fukubayashi T, Kurosawa H. The contact area and pressure distribution pattern of the knee: a study of normal and osteoarthrotic knee joints. *Acta Orthop Scand*. 1980;51:871-879.
9. Griffith CJ, LaPrade RF, Fritts HM, Morgan PM. Posterior root avulsion fracture of the medial meniscus in an adolescent female patient with surgical reattachment. *Am J Sports Med*. 2008;36:789-792.
10. Harner CD, Mauro CS, Lesniak BP, Romanowski JR. Biomechanical consequences of a tear of the posterior root of the medial meniscus: surgical technique. *J Bone Joint Surg Am*. 2009;91:257-270.
11. Kim JG, Lee YS, Bae TS, et al. Tibiofemoral contact mechanics following posterior root of medial meniscus tear, repair, meniscectomy, and allograft transplantation. *Knee Surg Sports Traumatol Arthrosc*. 2013;21:2121-2125.
12. Kim SB, Ha JK, Lee SW, et al. Medial meniscus root tear refixation: comparison of clinical, radiologic, and arthroscopic findings with medial meniscectomy. *Arthroscopy*. 2011;27:346-354.
13. Kocabey Y, Taser O, Nyland J, et al. Horizontal suture placement influences meniscal repair fixation strength. *Knee Surg Sports Traumatol Arthrosc*. 2013;21:615-619.
14. Kopf S, Colvin AC, Muriuki M, Zhang X, Harner CD. Meniscal root suturing techniques: implications for root fixation. *Am J Sports Med*. 2011;39:2141-2146.
15. Kurosawa H, Fukubayashi T, Nakajima H. Load-bearing mode of the knee joint: physical behavior of the knee joint with or without menisci. *Clin Orthop Relat Res*. 1980;149:283-290.
16. Lee DW, Jang SH, Ha JK, Kim JG, Ahn JH. Meniscus root refixation technique using a modified Mason-Allen stitch. *Knee Surg Sports Traumatol Arthrosc*. 2013;21:654-657.
17. Lee YH, Nyland J, Burden R, Caborn DN. Repair of peripheral vertical meniscus lesions in porcine menisci: in vitro biomechanical testing of 3 different meniscus repair devices. *Am J Sports Med*. 2013;41(5):1074-1081.
18. Matsubara H, Okazaki K, Izawa T, et al. New suture method for radial tears of the meniscus: biomechanical analysis of cross-suture and double horizontal suture techniques using cyclic load testing. *Am J Sports Med*. 2012;40(2):414-418.
19. Mitchell R, Matava M, Pitts R, Kim YM. Medial meniscus root avulsion: a biomechanical comparison of four different repair constructs. *Arthroscopy*. 2013;29(6):e32.
20. O'Connor BL, McConaughy JS. The structure and innervation of cat knee menisci, and their relation to a "sensory hypothesis" of meniscal function. *Am J Anat*. 1978;153:431-442.
21. Petersen W, Zantop T. Avulsion injury to the posterior horn of the lateral meniscus: technique for arthroscopic refixation. *Unfallchirurg*. 2006;109:984-987.
22. Ponce BA, Hosemann CD, Raghava P, Tate JP, Sheppard ED, Eberhardt AW. A biomechanical analysis of controllable intraoperative variables affecting the strength of rotator cuff repairs at the suture-tendon interface. *Am J Sports Med*. 2013;41(10):2256-2261.
23. Shoemaker SC, Markolf KL. The role of the meniscus in the anterior-posterior stability of the loaded anterior cruciate-deficient knee: effects of partial versus total excision. *J Bone Joint Surg Am*. 1986;68:71-79.
24. Starke C, Kopf S, Lippisch R, Lohmann CH, Becker R. Tensile forces on repaired medial meniscal root tears. *Arthroscopy*. 2013;29:205-212.
25. Vyas D, Harner CD. Meniscus root repair. *Sports Med Arthrosc*. 2012;20:86-94.